

# Behaviour of the spin–spin relaxation time for natural rubber vulcanizates under large deformation

Hidetoshi Oikawa and Kenkichi Murakami

Chemical Research Institute of Non-Aqueous Solutions, Tohoku University, Sendai 980 Japan

(Received 17 December 1981; revised 10 February 1982)

The spin–spin relaxation time,  $T_2$ , for DCP-cured natural rubber with various crosslink densities,  $\nu_e$ , has been measured under various deformation.  $T_2$  is separated into two components: one is the long  $T_2$  component,  $T_{2L}$ , for the mobility of amorphous network chains, the other is the short one,  $T_{2S}$ , for that of the strain-induced crystalline chains.  $T_{2L}$  decreased exponentially with increasing extension ratio,  $\alpha$ , and the decreasing rate was more remarkable with increasing  $\nu_e$ . The  $\alpha$  and  $\nu_e$  dependence of  $T_{2L}$  has been quantitatively explained by the equation experimentally derived by Nishi *et al.*  $T_{2L}$  under various extension increased and became almost constant with increasing temperature, while the corrected fraction of  $T_{2S}$ ,  $T_{2S}(\%)$ , gradually decreased. The apparent melting point,  $T_m$ , at which the corrected  $T_{2S}(\%)$  was zero under various deformation was determined. The  $\alpha$  dependence of  $T_m$  has been discussed by using Flory's equation.

**Keywords** Pulsed nuclear magnetic resonance; spin–spin relaxation time; natural rubber vulcanizates; strain-induced crystalline; dipolar interaction; enthalpy of fusion

## INTRODUCTION

The relationship between the spin–spin relaxation time,  $T_2$ , and the crosslink density,  $\nu_e$ , for rubber vulcanizates has been studied in detail<sup>1</sup>.  $T_2$  is related to long range motions of network chains between the two crosslinkages and is influenced by such factors as molecular weight and crosslink density as well as temperature.

Manufactured goods made from rubber are often used under large strain. Behaviour of rubber vulcanizates under large deformation is very important not only from the industrial point of view but also from the fundamental scientific view point, but has not been completely explained theoretically.

Most experiments under high extension were either the stress–strain and/or stress–relaxation method<sup>2</sup> or structural analysis by using X-ray diffraction methods<sup>3</sup>. However, since molecular motions are not influenced or perturbed by the applied static magnetic field, reliable information about the mobility of network chains can be expected from n.m.r. for elastomers under deformation. However, there are some drawbacks in the measurements and analyses by broad-line n.m.r. (rapid-passage n.m.r.)<sup>4</sup> as suggested by Nishi *et al.*<sup>5</sup>

In this article the solid echo technique<sup>5,6</sup>, the pulse sequence of which is  $90^\circ_x, \tau, 90^\circ_y$ , has been applied. The dependence of extension ratio,  $\alpha$ ,  $\nu_e$  and temperature on  $T_2$  for rubber vulcanizates under deformation and the crystallinity of the strain-induced crystalline have been discussed.

## EXPERIMENTAL

The cylindrical samples of crosslinked natural rubber (NR) were prepared by milling 3 phr of DCP (dicumyl

peroxide) with uncrosslinked rubber followed by pressing at 145°C and 200 kg cm<sup>-2</sup> for given intervals. All the samples were extracted with hot acetone for 48 h in order to eliminate the impurities and were dried *in vacuo*.

The cylindrical samples were cut into round slices and fixed at constant strain around the outside of the glass rod. The rod has the groove on each end.  $\alpha$  was determined by the ratio of the length around the rod to the circumference of a band rubber sample<sup>7</sup>.

The crosslink densities,  $\nu_e$ , for all samples are given in the last column of *Table 1*.  $\nu_e$  was determined by the equilibrium degree of swelling for vulcanized NR samples swollen in toluene at 30°C and using the Flory–Rehner equation.

A pulsed-n.m.r. spectrometer was used to measure  $T_2$  (Bruker-CXP type) with a proton resonance frequency of 90 MHz. The direction of extension and the applied static magnetic field were perpendicular to each other. The pulse sequence was  $90^\circ_x, \tau, 90^\circ_y$ . The width of the  $90^\circ$  pulse and the  $\tau$ -value were 2  $\mu$ s and 10  $\mu$ s, respectively. The  $T_2$  measurements have been carried out on three kinds of DCP-cured NR in the temperature range from room temperature to 373.15 K. The samples to be measured were placed in the probe at the correct temperature and left for 20–30 min to ensure equilibrium.

## RESULTS AND DISCUSSION

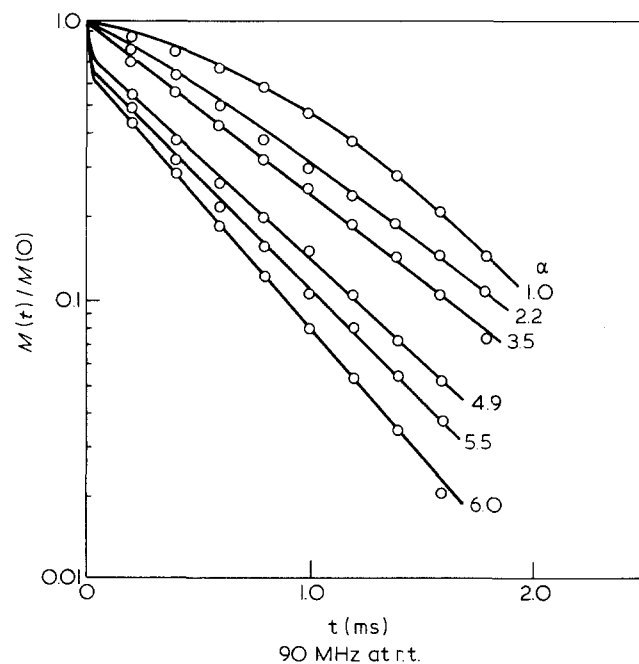
*Figure 1* shows the relative signal strength of solid echo,  $M(t)/M(0)$ , for sample C measured under various extensions at room temperature. The solid echo can be approximately regarded as the free induction decay (FID) after  $90^\circ$  pulse<sup>6</sup>. The decay of  $M(t)/M(0)$  is more rapid with increasing  $\alpha$ , which means  $T_2$  for an extended sample

**Table 1** Preparation of natural rubber vulcanizates and the crosslink densities for all samples

Sample	DCP*	Curing time (min)	$10^2 \nu_e$ (mol dm <sup>-3</sup> )
A	3 phr†	20	4.23
B	3	30	5.50
C	3	40	6.66

\* Dicumyl peroxide

† Parts per hundred rubber

**Figure 1** The change of the relative signal strength of solid-echo,  $M(t)/M(0)$ , measured for sample C under various extension ratio,  $\alpha$ , at room temperature

becomes shorter. The Kubo-Tomita equation describes the molecular motional narrowing by<sup>8</sup>:

$$M(t)/M(0) = \exp[-\sigma_0^2 \tau_c \{ \exp(-t/\tau_c) + (t/\tau_c) - 1 \}] \quad (1)$$

where  $\tau_c$  is the correlation time of molecular motion, and  $\sigma_0^2$  means the second moment of the resonance.

Equations (2) and (3) are derived from equation (1). The former is at  $\tau_c < 10^{-6}$  s and the latter at  $\tau_c > 10^{-5}$  s.

$$M(t)/M(0) = \exp(-\sigma_0^2 \tau_c t) \equiv \exp(-t/T_2) \quad (2)$$

$$M(t)/M(0) = \exp(-\sigma_0^2 t^2/2) \equiv \exp(-t^2/2T_2^2) \quad (3)$$

However, as shown in *Figure 1* the actual  $M(t)/M(0)$  did not decay exponentially. The  $M(t)/M(0)$  under undeformed state or low extension decays non-exponentially because molecular motions are so rapid that the effect of chemical shift is no longer negligible<sup>9</sup>. On the other hand, the  $M(t)/M(0)$  under high extension than  $\alpha = 5$  decreased remarkably in short time region due to the strain-induced crystallization. So,  $T_2$  under free state or low extension was determined by the Weibull type function expressed by<sup>9,10</sup>:

$$M(t)/M(0) = \exp\left\{-\frac{1}{\mu} \left(\frac{t}{T_2}\right)^\mu\right\} \quad 1 \leq \mu \leq 2 \quad (4)$$

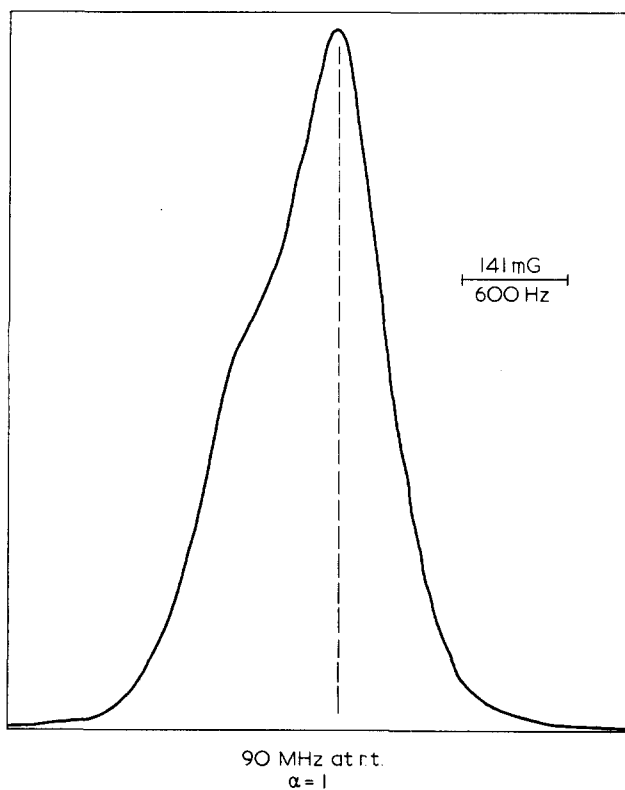
where  $\mu$  is the distribution parameter of the n.m.r. line shape.  $T_2$  under high extension was calculated from equation (5) which was derived on the assumption of the additivity of equations (2) and (3)<sup>11</sup>.

$$M(t)/M(0) = f \exp(-t^2/2T_{2S}^2) + (1-f) \exp(-t/T_{2L}) \quad (5)$$

where  $f$  is the fraction of short  $T_2$  component,  $T_{2S}$ .

It is evident that the  $M(t)/M(0)$  under free state or small deformation is influenced by chemical shift as shown in *Figure 2*. *Figure 2* shows the absorption line of n.m.r. into which the solid echo signal for sample C at  $\alpha = 1$  was converted by Fourier transformation. If equations (2) and (3) are converted by Fourier transformation, the former becomes Lorentzian and the latter Gaussian type function. However, the n.m.r. line shape in *Figure 2* is neither Lorentzian nor Gaussian type. Thus, the width of line shape is apparently broadened due to chemical shift<sup>9</sup>. As a result, the  $M(t)/M(0)$  decays non-exponentially, even if the  $\tau_c$  of NR chains is in the range of the motional narrowing.

*Figure 3* shows the change of  $T_2$  under various extension. The long  $T_2$  component,  $T_{2L}$ , and the short one,  $T_{2S}$ , correspond to the mobility of amorphous network chains and to the strain-induced crystalline chains, respectively. The  $T_{2S}$  was clearly observed at higher extension ratio than  $\alpha = 4$  and independent of  $\alpha$ . Because  $T_{2S}$  is independent of  $\tau_c$  and takes the constant as expressed by equation (3) since  $\tau_c$  of the crystalline chains is longer than  $10^{-5}$  s. The  $T_{2L}$  in the range of  $\alpha = 3$  to 5 usually varied to some extent. It is thought that when the strain-induced crystallization occurs under intermediate deformation the motion or the degree of strain of amorphous network chains is more or less different from one another, even though  $\alpha$  is macroscopically the same.

**Figure 2** The n.m.r. absorption line for sample C in free state at room temperature

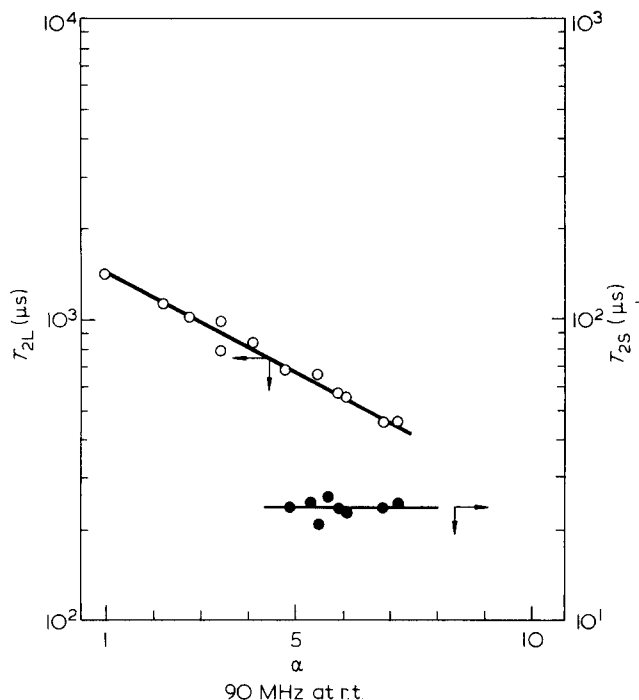


Figure 3 The  $\alpha$  dependence of  $T_{2L}$  and  $T_{2S}$  for sample B at room temperature:  $T_{2L}$  is a long component of  $T_2$  for the mobility of amorphous network chains;  $T_{2S}$  is a short one for that of the strain-induced crystalline chains

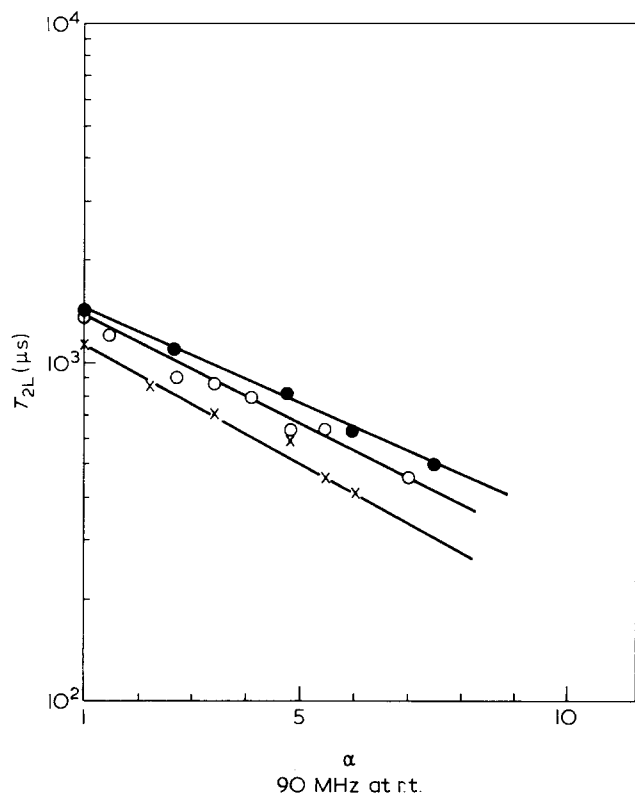


Figure 4 The  $\alpha$  dependence of  $T_{2L}$  for samples at room temperature with various crosslink densities,  $10^2 v_e$  (mol dm $^{-3}$ ): ●, 4.226; ○, 5.504; X, 6.657

This result suggests that the original network is inhomogeneous.

Figure 4 shows the  $v_e$  dependence of  $T_{2L}$  decreased exponentially with increasing  $\alpha$ , and the decreasing rate of  $T_{2L}$  increased with  $v_e$ . Since it is known that  $\sigma_0^2$  is almost independent of deformation, the decreasing of  $T_{2L}$  is

explicable to be caused by the  $\tau_c$  dependence on  $\alpha$  as expressed by equation (2)<sup>12</sup>. Thus, the  $\tau_c$  of micro-Brownian motion of network chains becomes longer with extension. Nishi *et al.* reported the experimental relation among  $T_{2L}$ ,  $\alpha$  and  $v_e$  by<sup>7</sup>:

$$T_{2L}(\alpha, v_e) = T_{2L}(\alpha = 1, v_e) \exp\{-K(v_e)(\alpha - 1)\} \quad (6)$$

The results in Figure 4 could be described by equation (6). The  $v_e$  dependence of  $K(v_e)$  is shown in Figure 5. Although the number of plots in Figure 5 was three, the straight line was drawn by the least-square fitting, which is represented by:

$$K(v_e) = -4.82 \times 10^{-3} + 3.14 v_e \quad (7)$$

Equation (7) can be adequately approximated to equation (8) within experimental errors.

$$K(v_e) \approx 3.14 v_e \quad (8)$$

It is found that  $K(v_e)$  for unvulcanized rubber samples (at  $v_e = 0$ ) is zero from equation (8). That is,  $T_{2L}(\alpha, v_e = 0)$  is equal to  $T_{2L}(\alpha = 1, v_e = 0)$ , which agrees with the fact that the deformation of uncured rubber generally occurs not because of the extension of molecular chains but because of the slippage among them. Nishi *et al.* reported the result as expressed by equation (9) from  $T_2$  measurements for accelerated-sulphur cured NR<sup>7</sup>:

$$K(v_e) \approx 1.12 v_e \quad (9)$$

The coefficient in equation (8) is roughly three times that in equation (9). The cause of which is not determined.

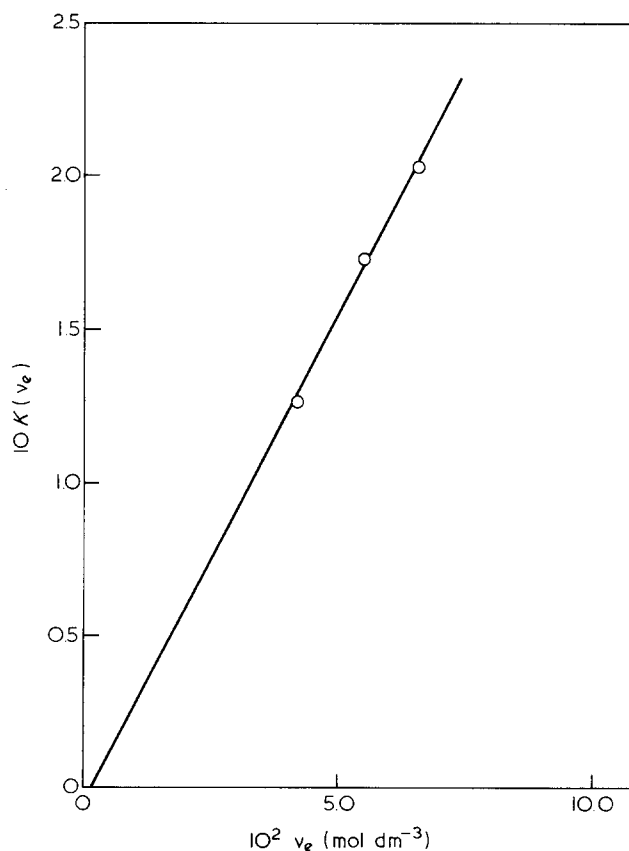


Figure 5 Plot of  $K(v_e)$  vs.  $v_e$

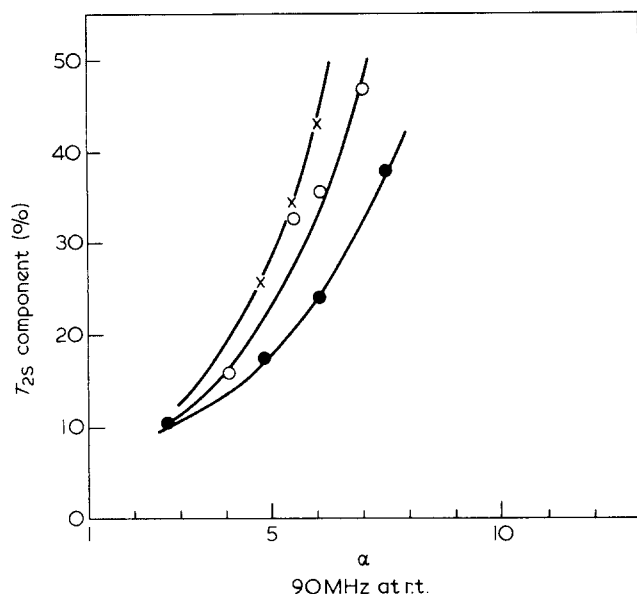


Figure 6 The  $\alpha$  dependence of the fraction of  $T_{2S}$ ,  $T_{2S}$  (%), for samples at room temperature with various crosslink densities,  $10^2 \nu_e$  (mol dm $^{-3}$ ): ●, 4.226; ○, 5.504; X, 6.657

However, it may be interesting if the difference is based upon the distinction between the two vulcanization systems.

Figure 6 shows the fraction of  $T_{2S}$ ,  $T_{2S}$ (%), i.e.  $f$  in equation (5), dependence on  $\alpha$  and  $\nu_e$ .  $T_{2S}$ (%) increased remarkably with  $\alpha$  and  $\nu_e$ . There was several per cent of  $T_{2S}$ (%) at  $\alpha=1$  due to the impurities which could not be eliminated by extraction or due to the inhomogeneities in the network. In our case  $\tau_c$  at which the motional narrowing occurs is ca.  $10^{-5}$  s, and the  $\tau_c$  of NR at room temperature is in the range of  $10^{-7}$  to  $10^{-8}$  s. If one takes off the values of  $T_{2S}$ (%) at  $\alpha=1$  from the observed  $T_{2S}$ (%) under deformation, the values of corrected  $T_{2S}$ (%) can be regarded as crystallinity, and are roughly close to the crystallinity measured by X-ray diffraction method<sup>13</sup>.

Figure 7 shows the temperature dependence of  $T_2$  at  $\alpha=1$ , 6.897 and 7.118. At any extension,  $T_{2L}$  increased at lower temperature region and became almost constant above 350 K, while  $T_{2S}$  was independent of temperature.  $T_2$  is constant below  $T_g$ . The plateau of  $T_{2L}$  at higher temperature as seen from Figure 7 resembles solid-like behaviour in spite of  $\tau_c < 10^{-6}$  s. This reflects the incomplete averaging of dipolar interactions due to the anisotropic motions of network chains. Not only the high frequency motions of short sections of chains but also the low frequency motions over the wide range of chains must be averaged out in order to eliminate the anisotropic motions. In other words, the form of spin-spin relaxation decay is attributed to the existence of residual unaveraged dipolar interactions which confer a pseudo solid-like response on the spin-spin relaxation. The low frequency motions, however, are constrained because of the chemical crosslinkages or entanglements in the network. So, those motions are highly complex owing to the multiplicity of types of motions<sup>14</sup>. These long range or lower frequency motions have great influence on  $T_2$ . Probably, this effect is thought to be more remarkable under higher extension. Consequently, the value of  $T_{2L}$  under free state or small deformation becomes a sensitive index of the crosslink density.

McCall and Anderson have discussed the mobility of amorphous and crystalline chains in polyethylene<sup>15</sup>. Their results are

$$T_2 \approx \frac{1}{\gamma \Delta H_{1/2}} \approx \frac{\mu}{r^3} \cos \theta_0 \sin^2 \theta_0 \quad (10)$$

where  $\gamma$ ,  $\mu$  and  $r$  are the proton gyromagnetic ratio, the nuclear magnetic moment and the internuclear distance, respectively. Thus, the ratio of the narrow resonance width to the rigid lattice width is of the order of  $\cos \theta_0 \sin^2 \theta_0$ .  $\theta_0$  is the angle between the internuclear vector and the applied static magnetic field, and evaluated from the experiment. It was assumed that the arbitrarily rapid molecular motions were restricted under  $\theta > \theta_0$ . So their results may be applied to our case, and equation (11) can be derived.

$$T_{2S}/T_{2L} \approx \cos \theta_0 \sin^2 \theta_0 \quad (11)$$

$\theta_0$  was  $\sim 12^\circ$  in case of  $\alpha=7.118$ . The value at 350 K was used as  $T_{2L}$ . This value of  $\theta_0$  is much closer to the one ( $\theta_0 \approx 13^\circ$ ) determined by the ratio of the narrow resonance width for amorphous chains to rigid-lattice width for chains bound on the surface of carbon black in polybutadiene-carbon black mixture<sup>11</sup>. The morphology of the strain-induced crystalline chains is different from that of the bound rubber, however, from the view point of molecular motions it is found that both of the segments in the above two kinds of chains are restrained to the same extent.

The 'X'-marks in Figure 7 mean  $\mu$ -value for sample B at  $\alpha=1$ . The averaged one was  $\sim 1.34$ .

The change of corrected  $T_{2S}$ (%) with increasing temperature under various extension ratios is shown in Figure 8. The temperature at which corrected  $T_{2S}$ (%) was zero was defined as the apparent melting point,  $T_m$ .  $T_m$  became higher with  $\alpha$  as seen from Figure 8. Table 2 listed the enthalpy of fusion per monomeric unit,  $\Delta H_u$ , calculated according to equation (12)<sup>16</sup>, assuming that  $T_m$

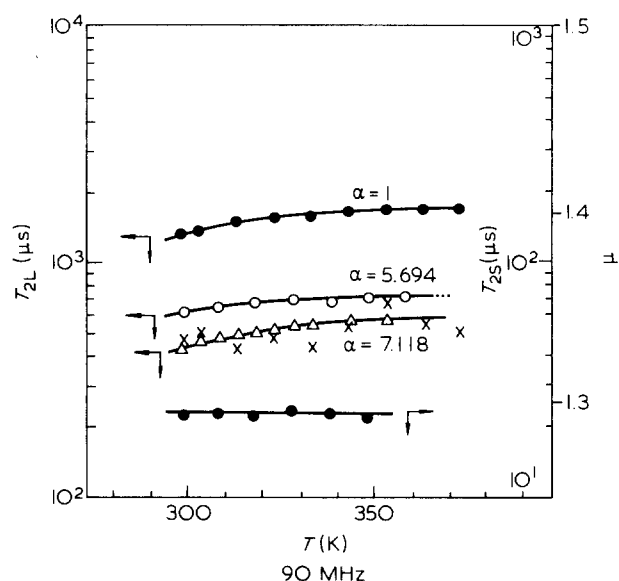


Figure 7 The temperature dependence of  $T_{2L}$  and  $T_{2S}$  for sample B under various extension. The 'X'-marks mean the change of  $\mu$ -values in equation (5) with increasing temperature for sample B in free state

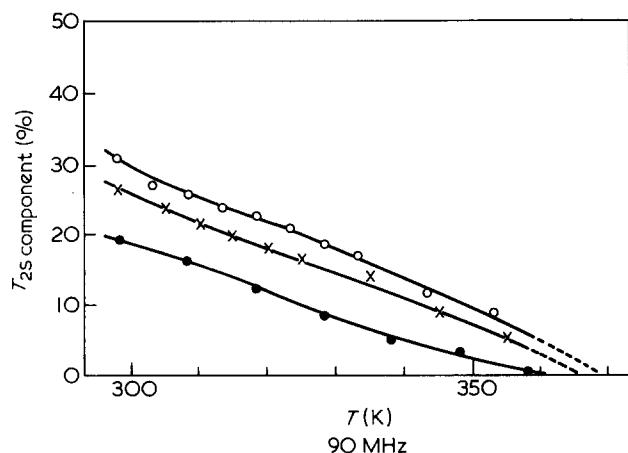


Figure 8 The change of corrected  $T_{2S}$  (%) with increasing temperature for sample B under various extension,  $\alpha$ :  $\circ$ , 7.118;  $\times$ , 6.897;  $\bullet$ , 5.694

Table 2 The list of  $T_m^0$  and  $\Delta H_u$  determined by various methods

	$T_m^0$ (K)	$\Delta H_u$ (kJ mol $^{-1}$ )
n.m.r.	318.18 <sup>a</sup> , 309.17 <sup>b</sup>	7.90 <sup>a</sup> , 7.70 <sup>b</sup>
s.m.m. <sup>c</sup>	289.15 <sup>d</sup>	4.92 <sup>d</sup>
f.p.d. <sup>e</sup>	301	4.37 $\pm$ 0.25

<sup>a</sup>  $N_u = 85.1$ ,  $S = 1.5$

<sup>b</sup>  $N_u = 158$ ,  $S = 1.5$

<sup>c</sup> Stress measurement method (ref. 16)

<sup>d</sup>  $N_u = 291$ ,  $S = 1.5$

<sup>e</sup> Freezing point depression method (ref. 17)

can be regarded as the thermodynamically equilibrium one under deformation.

$$\frac{1}{T_m} = \frac{1}{T_m^0} - \frac{R}{2N_u\Delta H_u} F(\alpha) \quad (12)$$

$$F(\alpha) = \left(\frac{24N}{\pi}\right)^{1/2} - \left(\alpha^2 + \frac{2}{\alpha}\right)$$

$$N = N_u/S$$

where  $F(\alpha)$ ,  $R$ ,  $N_u$  and  $S$  are the strain function, the gas constant, the number of monomeric unit between the two crosslinkages and the number of monomeric unit per statistical chain segment, respectively.  $N_u$  of sample B is 85.1 from swelling method, and is 158 from stress-strain measurement.  $S$  is 1.5 (ref 17). In Table 2,  $T_m^0$  and  $\Delta H_u$  determined by n.m.r. experiment are higher than those by stress measurement<sup>18</sup> or freezing point depression method<sup>19</sup>. In particular,  $\Delta H_u$  is approximately twice as much as the other  $\Delta H_u$ . Some causes can be considered. Firstly, since equation (12) was derived on the basis of the Gaussian network, it is incorrect to analyse the n.m.r. experimental data measured under large deformation by using equation (12). Secondly, the parameters of  $N_u$  and  $S$  are doubtful. Assuming that the values of  $\Delta H_u$  and  $T_m^0$  are 4.65 kJ mol $^{-1}$  and 295 K, respectively, as shown in Table 2, if one calculates  $S$  from equation (12) by using the obtained experimental data in this study,  $S$  is  $\sim 2.4$ . The above value of  $S$  has not been proved by any other method. However, the main reason may be that the  $T_m$  under

deformation is not essentially the real equilibrium one. Because the new thermodynamically equilibrium state is probably achieved due to fusion and crystallization of the strain-induced crystalline during the  $T_2$  measurements at each temperature.  $T_m^0$  and  $\Delta H_u$  were recalculated according to corrected equation (12); the strain function in equation (12) was replaced by the one based upon the non-Gaussian network. However, the recalculated values of  $T_m^0$  and  $\Delta H_u$  did not agree with those obtained from the other methods in Table 2. The above result supports the idea that  $T_m$  is not the equilibrium melting point under deformation. This point must be clarified in future work.

## CONCLUSION

$T_2$  ( $T_{2L}$  and  $T_{2S}$ ) for DCP-cured NR has been measured under deformation. It was found that  $\alpha$  and  $v_e$  dependence of  $T_{2L}$  was quantitatively explicable on the basis of the experimental equation reported by Nishi *et al.*<sup>7</sup> However, the  $v_e$  dependence of the constant,  $K(v_e)$ , in the above equation for DCP-vulcanization was more remarkable than that for the accelerated-sulphur vulcanization.  $T_{2L}$  under various extension at higher temperature than 350 K was almost constant, since the dipolar interactions are not completely averaged for the anisotropic motions of network chains due to the chemical crosslinkages and/or entanglement. The corrected  $T_{2S}$  (%) decreased with increasing temperature, and the apparent melting point,  $T_m$ , under deformation was estimated. The relationship between  $T_m$  and  $\alpha$  could not be explained quantitatively.

## ACKNOWLEDGEMENT

The authors are sincerely grateful to Mr. T. Miyazaki (Research and Development Division, Bridgestone Tire Co., Ltd.) for measuring the spin-spin relaxation time and for his many useful suggestions.

## REFERENCES

- Munie, G. C. and Jonas, J. J. *Polym. Sci., Polym. Chem. Edn.* 1981, **18**, 1061; Folland, R. and Charlesby, A. *Polymer* 1979, **20**, 207
- Su, T. K. and Mark, J. E. *Macromolecules* 1977, **10**, 120
- Field, J. E. *J. Appl. Phys.* 1941, **12**, 23
- von Meerwall, E., Creel, R. B., Griffin, C. F., Dicato, E., Lin, F. T. and Lin, F. M. *J. Appl. Polym. Sci.* 1977, **21**, 1489
- Fujimoto, K., Nishi, T. and Kado, R. *Polym. J.* 1972, **3**, 448; Nishi, T. *Rubb. Chem. Technol.* 1978, **51**, 1075
- Mansfield, P. *Phys. Rev.* 1965, **137**, A-961
- Nishi, T. and Chikaraishi, T. *J. Macromol. Sci.-Phys.* 1981, **B19(3)**, 445
- Kubo, R. and Tomita, K. *J. Phys. Soc. Jpn.* 1954, **9**, 888
- Fujimoto, K. and Nishi, T. *J. Soc. Rubb. Ind. Jpn.* 1972, **45**, 828; Fujimoto, K. and Nishi, T. *ibid.* 1970, **43**, 465
- Weibull, W. *J. Appl. Mech.* 1951, **73**, 293; Kaufman, S. and Bunger, D. J. *J. Magn. Resonance* 1970, **3**, 217
- Kaufman, S., Slichter, W. P. and Davis, D. D. *J. Polym. Sci. A-2* 1971, **9**, 829
- Chujo, R. *J. Soc. Rubb. Ind. Jpn.* 1958, **31**, 430
- Tanaka, Y. unpublished data
- Folland, R., Steven, J. H. and Charlesby, A. *J. Polym. Sci., Polym. Phys. Edn.* 1978, **16**, 1041
- McCall, D. W. and Anderson, E. W. *J. Polym. Sci.* 1963, **A-1**, 1175
- Flory, P. J. *J. Chem. Phys.* 1947, **15**, 397
- Treolar, L. R. G. 'The Physics of Rubber Elasticity', Oxford Univ. Press, 1958
- de Candia, F., Romano, G. and Vittoria, V. *J. Polym. Sci., Polym. Phys. Edn.* 1973, **11**, 229
- Roberts, D. E. and Mandelkern, L. *J. Am. Chem. Soc.* 1955, **77**, 781